Institutional Repository - Research Portal
Dépôt Institutionnel - Portail de la Recherche
researchportal.unamur.be
University of Namur

RESEARCH OUTPUTS / RÉSULTATS DE RECHERCHE

Linear and Nonlinear Optical Effects in Biophotonic Structures using Classical and Nonclassical Light

Verstraete, Charlotte; Mouchet, Sébastien R; Verbiest, Thierry; Kolaric, Branko

Published in:
Journal of biophotonics

DOI:
10.1002/jbio.201800262

Publication date:
2019

Document Version
Peer reviewed version

Link to publication

Citation for pulished version (HARVARD):
Verstraete, C, Mouchet, SR, Verbiest, T & Kolaric, B 2019, 'Linear and Nonlinear Optical Effects in Biophotonic Structures using Classical and Nonclassical Light', *Journal of biophotonics*, vol. 12, no. 1, e201800262, pp. e201800262. https://doi.org/10.1002/jbio.201800262

General rights
Copyright and moral rights for the publications made accessible in the public portal are retained by the authors and/or other copyright owners and it is a condition of accessing publications that users recognise and abide by the legal requirements associated with these rights.

- Users may download and print one copy of any publication from the public portal for the purpose of private study or research.
- You may not further distribute the material or use it for any profit-making activity or commercial gain
- You may freely distribute the URL identifying the publication in the public portal ?

Take down policy
If you believe that this document breaches copyright please contact us providing details, and we will remove access to the work immediately and investigate your claim.

Download date: 16. Jul. 2024

Accepted Article

Linear and Nonlinear Optical Effects in Biophotonic Structures using Classical and Nonclassical Light

Charlotte Verstraete[1], **Sébastien R. Mouchet**[2,3,*], **Thierry Verbiest**[1], **and Branko Kolaric**[4,5,6**]

[1]Molecular Imaging and Photonics, Department of Chemistry, KU Leuven, Celestijnenlaan 200D, 3001 Heverlee, Belgium

[2]School of Physics, University of Exeter, Stocker Road, Exeter EX4 4QL, United Kingdom

[3]Department of Physics & Namur Institute of Structured Matter (NISM), University of Namur, Rue de Bruxelles 61, 5000 Namur, Belgium

[4]Micro- and Nanophotonic Materials Group, University of Mons, Place du Parc 20, 7000 Mons, Belgium

[5]Center for Photonics, Institute of Physics, University of Belgrade, Pregrevica 118, 11080, Belgrade, Serbia

[6]Old World Labs, 1357 N. Great Neck Road Suite 104, Virginia Beach, VA 23454, USA

*s.mouchet@exeter.ac.uk **branko.kolaric@umons.ac.be

Abstract

In this perspective article, we review the optical study of different biophotonic geometries and biological structures using classical light in linear and nonlinear regime, especially highlighting the link between these morphologies and modern biomedical research. Additionally, the importance of nonlinear optical study in biological research, beyond traditional cell imaging is also highlighted and described. Finally, we present a short introduction regarding nonclassical light and describe the new future perspective of quantum optical study in biology, revealing the link between quantum realm and biological research.

1 Introduction

It has been known for a long time that colors in nature are not merely there for beauty, but are of the utmost importance for communication. Both intra- and interspecies communication can occur thanks to colors, e.g., for sexual communication or to warn potential predators. The biological relevance of colors can thus not be underestimated because of the role of visual appearance in natural selection. Examples that definitely come to mind when thinking about colorful natural specimens, are butterflies and beetles. As butterflies and many beetles have the ability to fly over extremely long distances, a lot of species have evolved in different geographical locations, and thus large variations in color can be observed between species and subspecies [1, 2, 3].

Other examples in nature highlighting the important role of colors are flowers. In general, flowers are reproducing thanks to pollinators carrying around pollen from one flower to another. By displaying distinctive colors, flowers can appear more attractive and recognizable to such pollinating insects. Additionally, flowers that do not offer floral rewards (e.g., nectar or protein-rich pollen), can opt to mimic colors of rewarding flowers and therefore misleading the pollinators [4]. Many species have therefore developed efficient vision systems able to distinguish different colors [1].

Natural colors can originate from either chemical or physical properties, or both combined. Colors of chemical origin are caused by colorful pigments and dyes, while physical colors originate from light interference. The latter, which is developed into further detail in this review, is due to the interaction of visible light, the wavelength of which is in the order of several hundreds of nanometers, with nanometer-scale features of photonic structures. Chemical and physical colors are often easily distinguishable, as pigments can be photobleached and their activity will decline over time, while structural colors cannot fade, unless the structure is somehow modified or damaged.

This article has been accepted for publication and undergone full peer review but has not been through the copyediting, typesetting, pagination and proofreading process, which may lead to differences between this version and the Version of Record. Please cite this article as doi: 10.1002/jbio.201800262

This article is protected by copyright. All rights reserved.

Accepted Article

Examples of natural structural colors are found in organisms [1] ranging from mammals such as primates (including humans's blue eyes) and marsupials [5, 6] or birds such as hummingbirds [7] and pigeons [8, 9] to insects such as butterflies [3] and beetles [2].

Some of the most common photonic structures in nature are photonic crystals. They comprise periodic photonic structures, with periods in the nanometer scale. Due to this periodicity in the same size-scale as the incident light, photonic crystals can be regarded as a medium that periodically changes refractive index in space from the incident light point of view. They can be probed with both classical and quantum light to unravel linear and nonlinear properties of these biological tissues. By investigating these properties, many insights can be obtained that could lead to the development of optical applications through a bioinspiration approach [10].

Nonlinear optical microscopy has been proven to be a very versatile and powerful technique, which shows many of the advantages of the classical optical microscopy, but without several of the disadvantages. Some important advantages of nonlinear optical microscopy are the increased imaging depth, and a strong reduction in photodamage. Additionally, Second Harmonic Generation (SHG) is an excellent tool to probe anisotropy and unravel the orientation of distinct structural features.

Beyond studying interaction of classical light with biological matter, the application of nonclassical or quantum light in biomedicine and biology is still at an infant stage of research. However, in this perspective article, we want to describe the essential features of quantum light to the broad biological community and to address the most significant advantages and challenges of using quantum light in biology, offering the possibility to move classical biological and biomedical studies into quantum realm.

2 Linear Optical Effects in Biophotonic Structures

The properties of light and interaction of light with matter are fully described by Maxwell's theory within the framework of classical electromagnetism [11]. From a classical point of view, an incident light beam may interact in three different ways with matter. It can either be transmitted, reflected or absorbed. These three phenomena play key roles in biological functions of natural organisms such as their visual appearances or thermal management.

One of the biological tissues optimized for light transmission is found in the transparent wings of insects such as cicada species in the order Hemiptera [12, 13, 14, 15]. These wings mostly consist of chitin, a polysaccharide that acts as building material for all insects. Both wing surfaces are covered by quasi-periodic arrays of hexagonally close-packed protrusions, which are at the origin of remarkable anti-reflective properties due to a mechanism of impedance matching between the wing material and air (Figure 1) [12, 13, 14]. This protrusion geometry and the related anti-reflective behavior are very similar for female and male as well as for many investigated cicada species [12, 13]. Over the optical range from 500 to 2500 nm, light transmittance of these wings rises over 90% and peaks at 98% [12, 13]. Within this wavelength range, which is larger than the lateral lattice parameter of the protrusion arrays, the transmission properties are not function of the microstructure morphology but the transmittance was found to depends linearly on the protrusion height [13]. These anti-reflective properties are believed to be related with camouflage against potential predators. Similar anti-reflective coatings were also found in other natural organisms such as the corneas of several insect eyes [16, 17] and the wings of *Cacostatia ossa* moth, *Cephonodes hylas* moth and butterflies from the *Greta* genus [18, 15, 19, 20, 21, 22, 23]. Due to their broad transparent window, these subwavelength nanostructures allowing to avoid unwanted light reflection were mimicked in order to design anti-reflective coatings for anti-glare glasses, screens, solar cells, light-sensitive detectors, camera lenses, telescopes or glass windows [24, 25]. Methods such as sol-gel processes, chemical vapor deposition, physical vapor deposition, etching processes, nanoimprint and biotemplate methods were used [24, 25]. In nature, biological surfaces are often multifunctional. They were optimized through evolution for different purposes [1]. In addition to anti-reflective properties, some cicada wings were found to exhibit (super-)hydrophobic [26, 13, 27, 14, 15] and anti-bacterial properties [28, 29, 30]. Dellieu and co-workers explained the interplay between the protrusion morphology, the anti-reflection and the hydrophobic properties [14, 15]: each protrusion can be modeled by a hemisphere covering a truncated cone. The latter plays a key role in the anti-reflective properties while the hemisphere is involved in the (super-)hydrophobic behavior of the wing surface. (Super-)hydrophobicity and antibacterial properties are important for many technological applications. Both behaviors are advantageous in the development of self-cleaning

This article is protected by copyright. All rights reserved.

Accepted Article

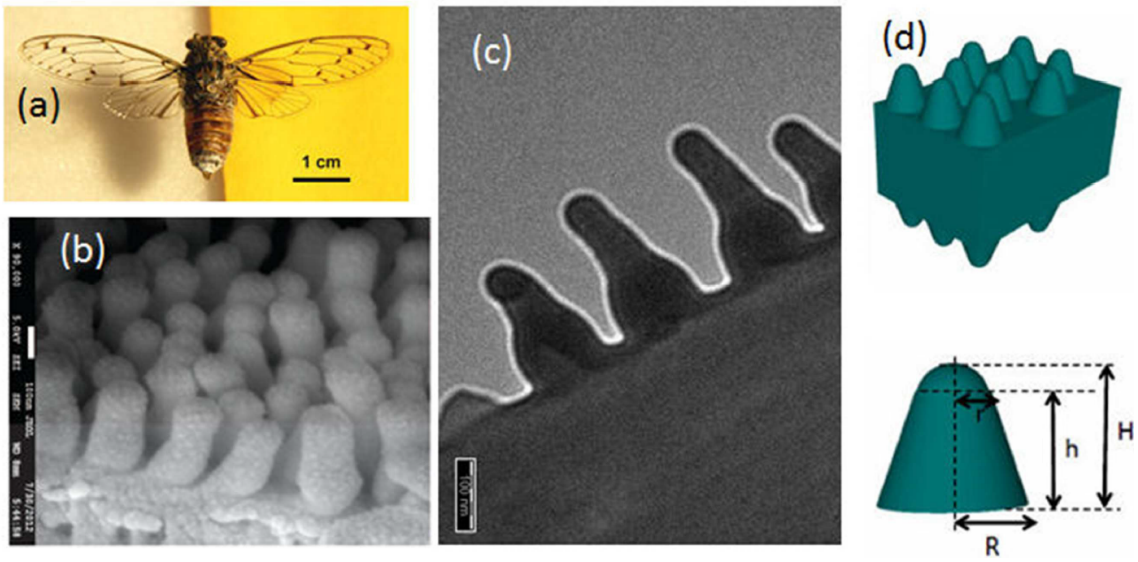

Figure 1: The grey *Cicada orni* (a) displays transparent wings, the anti-reflective properties of which are due to protrusions covering both wing surfaces (b,c). These protrusions were modeled by hemispheres covering truncated cones (d). Depending on the species, the spacing distance a_0 ranges between 40 and 200 nm, the protrusion diameter, between 40 and 150 nm and the height h, between 155 and 485 nm [12, 13, 14, 15]. In the case of *C. orni*, $r = 40$ nm, $R = 85$ nm, $H = 200$ nm and $h = 160$ nm. Reproduced from Deparis, O., Mouchet, S.R., Dellieu, L., Colomer, J.-F., Sarrazin, M., 2014. Nanostructured surfaces: bioinspiration for transparency, coloration and wettability. Mater. Today Proc. 1S, 122-129, with permission of Elsevier.

surfaces. From an industrial point of view, combining self-cleaning properties and antireflection thanks to only one single nanostructure is of high interest for instance in the fields of photovoltaics and solar absorbers [31].

Often, the visual appearance of natural organisms are however governed by light reflection and scattering. For instance, the fruits of *Margaritaria nobilis*, a tree, also known as bastard hogberry, found in the Caribbean, Mexico as well as Central and South America, exhibit bright iridescent green and blue colorations (Figure 2a,b) due to periodic photonic structures reflecting selectively incident circularly polarized light as a function of wavelength [32, 33]. After falling from the tree on the ground, the fruit and its green exocarp split, displaying the colorful endocarp. This visual appearance attracts birds, which disperse the seeds. In the cell walls of the fruit endocarp tissues, helicoidal plywood architectures, called Bouligand structures, give rise to light interference and strong reflection of circularly polarized light (Figure 2c-e). Within the cell's outer tissues, these helicoidal structures comprise concentrically-layered cellulose fibrils and have a period of about 180 nm [32, 33]. Such cells are stacked on each other in layers leading to an enhanced optical response. Inspired by these fruits' Bragg mirror combined with a cylindrical geometry, novel soft photonic fibers, which selectively scatter incident light in many directions, were developed by material scientists (Figure 2f-i) [32, 34]. These elastic polymer fibers exhibit an optical response, the hue of which is tuned by longitudinal mechanical strain (Figure 2j). Such bioinspired fibers have applications in the textile industry (for instance, in the development of anti-shirt-pulling jersey in sports), in optical strain sensing or in flexible photonic materials (e.g., smart surgical suture changing color when the right strain is applied) [32, 34].

If incident light is neither transmitted nor reflected upon interaction with matter, it is absorbed. In nature, photonic processes also contribute to the enhancement of light absorption. One of the most important light absorption mechanisms in living organisms occurs in plants and is related to photosynthesis. Recently, the photonic multilayer structures found in the blue iridescent epidermal chloroplasts of shade-dwelling *Begonia* leaves were demonstrated to enhance light harvesting for photosynthesis [35]. They comprise a periodic stack of absorbing thylakoid tissue. Through enhanced light trapping in the green range of the electromagnetic spectrum (corresponding to the forest canopy shade) and an increased quantum yield in low-light intensity environment, these leaves' photosynthesis is enhanced. Alternatively, conical microstructure covering various

This article is protected by copyright. All rights reserved.

Accepted Article

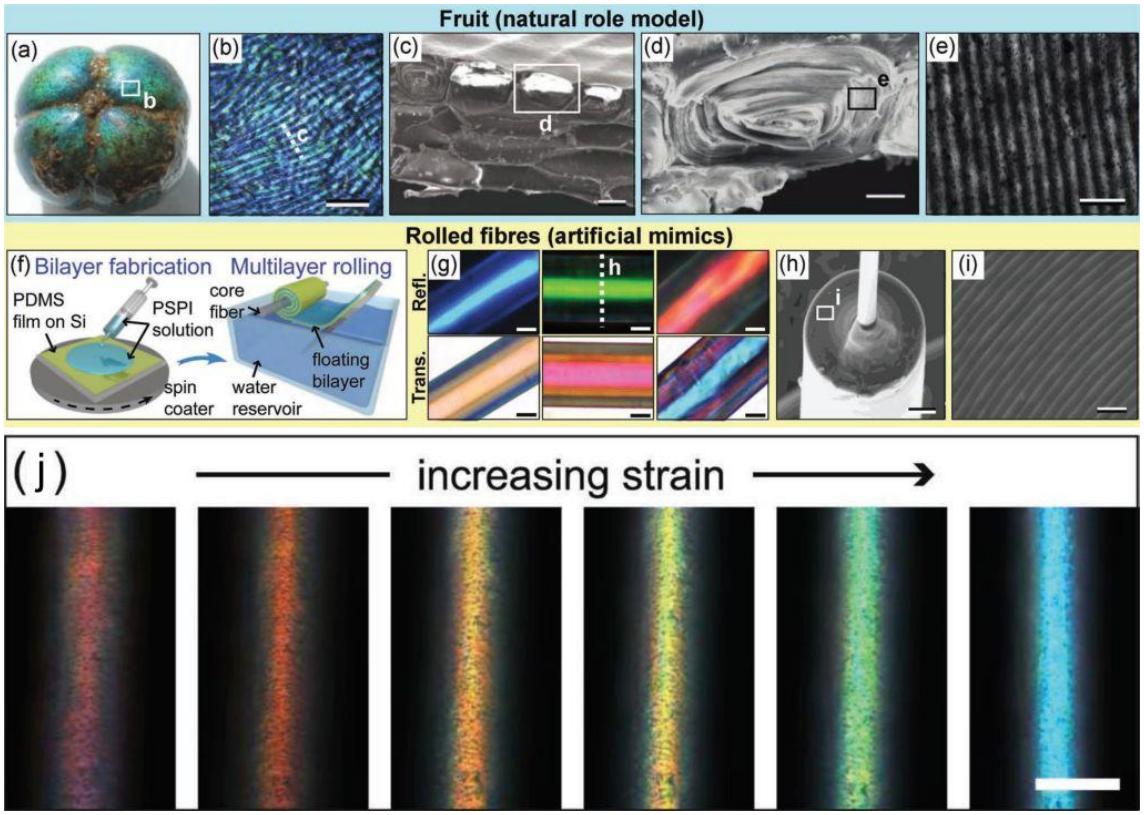

Figure 2: The endocarps of the fruits of *M. nobilis* exhibit green and blue colors (a,b) due to their tissues' cell walls (c,d) comprising Bouligand structures (e). Such structures were mimicked artificially by synthesizing planar periodic multilayers that were rolled in a water reservoir (f). Depending on the layer thicknesses, different colors are produced in reflection and transmission (g). Electron microscopy analyses of cross-sections of the mimicked photonic fibers allow to observe the rolled multilayer (h,i). Upon mechanical strain, the displayed color can be tuned in the entire visible spectrum (j). Scale bars: 200 μm (b), 20 μm (c), 10 μm (d), 500 nm (e), 20 μm (g), 20 μm (h), 1 μm (i) and 50 μm (j). Reproduced from Kolle M., Lethbridge, A., Kreysing, M., Baumberg, J. J., Aizenberg, J., Vukusic, P., 2013. Bio-Inspired Band-Gap Tunable Elastic Optical Multilayer Fibers. Adv. Mater. 25, 2239-2245, with permission of John Wiley and Sons.

This article is protected by copyright. All rights reserved.

Accepted Article

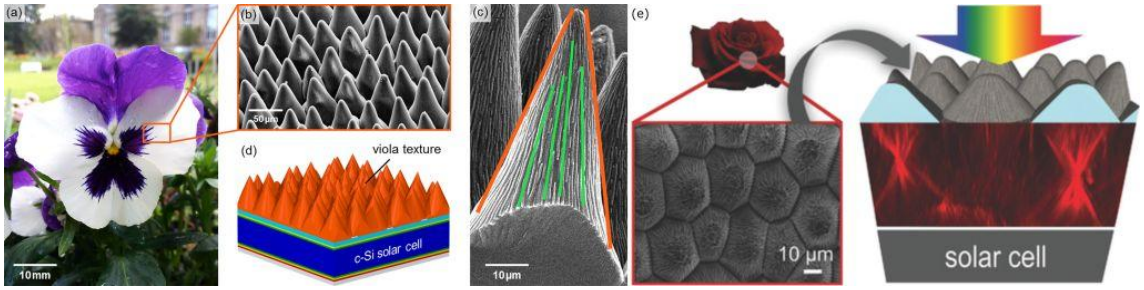

Figure 3: The petals of *Viola* and *Rosa* flowers (a,e) are covered by conical microstructurations (b,c,e) at the origin of enhanced light trapping properties. Coatings for solar cells can be inspired from such structures (d,e). Reproduced from (a-d) Schmager, R., Fritz, B., Hünig, R., Ding, K., Lemmer, U., Richards, B. S., Gomard, G., Paetzold, U. W., 2017. Texture of the *Viola* Flower for Light Harvesting in Photovoltaics. ACS Photon. 4, 2687-2692 and from (e) Hünig, R., Mertens, A., Stephan, M., Schulz, A., Richter, B., Hetterich, M., Powalla, M., Lemmer, U., Colsmann, A., Gomard, G., 2016. Flower Power: Exploiting Plants' Epidermal Structures for Enhanced Light Harvesting in Thin-Film Solar Cells, Adv. Optical Mater. 4, 1487-1493, with permission of (a-d) the American Chemical Society and (e) John Wiley and Sons, respectively.

plant textures such as petals and leaves (Figure 3a,e) were demonstrated to enhance light harvesting not only by anti-reflective properties, similarly to cicadas' wings, but also by combining the reduction of reflection losses and light focusing effects, following the redirection of incident photons [36, 37, 38, 39]. The cases of *Rosa* and *Viola* petals were specifically highlighted because of their high efficiencies (Figure 3a,e) [38, 39]. Such a combination of optical mechanisms leads to enhanced absorption for photosynthesis or strengthening of their color saturation, specifically under low-light conditions. In addition, these microstructures also give rise to superhydrophobic and self-cleaning behaviors [40, 41]. Because of their omnidirectional and broadband photonic properties, such photonic structures occurring in plants could lead to the development of novel designs for photovoltaics, solar absorbers and photocatalysis applications (Figure 3d,e).

Following incident light absorption, fluorescence emission can take place in natural organisms' integuments if fluorophores are present [42, 43, 44]. These molecules absorb higher-frequency photons (e.g., ultraviolet, violet or blue) and emit lower-frequency photons (e.g., in the visible range, from blue to red). This emission originates from electron transition between real states with the same spin multiplicity. Examples of such fluorescent molecules are the green fluorescent protein (GFP), psittacofulvin, biopterin and papiliochrome II. The resulting appearance may have biological functions in the visual communication of some organisms [43, 44]. When occurring in a photonic structure, emission from fluorophores is modified by the structure in terms of directivity and spectral intensity [45, 46]. Such a so-called controlled fluorescence takes place within the scales covering the elytra of the male *Hoplia coerulea* beetle (Figure 4a). In these scales, a photonic periodic multilayer (Figure 4b) is found giving rise to its blue-violet appearance (Figure 4c) [47, 48]. Fluorophores embedded within this multilayer emit a turquoise coloration (Figure 4d) under incident ultraviolet light [49, 50]. Both the color and the fluorescence emission are controlled by the photonic structure: upon contact with fluids, the fluorescence emission peak is observed to blue-shift, leading to a navy blue color (Figure 4f) [50, 48] whereas the reflectance peak wavelength undergoes a red-shift, giving rise to a green appearance (Figure 4f) [51, 52, 53, 54, 55], following liquid penetration into the scale structure and the filling of its air pores. Very recently, two-photon excitation fluorescence and Third-Harmonic Generation (THG) analyses (as detailed further in the next section) highlighted the multi-excited states character of *H. coerulea*'s fluorophores as well as the anisotropy of its photonic structure [56].

3 Nonlinear Optical Effects in Biophotonic Structures

In addition to the optical properties of biological materials collected by linear techniques, much supplementary information can be gathered with higher intensity laser beams. Such probes allow to characterize their nonlinear optical properties. At low light intensities the linear optical response of a molecule can be described by its induced dipole moment ($\boldsymbol{\mu}(\omega)$) that will oscillate with the

This article is protected by copyright. All rights reserved.

Accepted Article

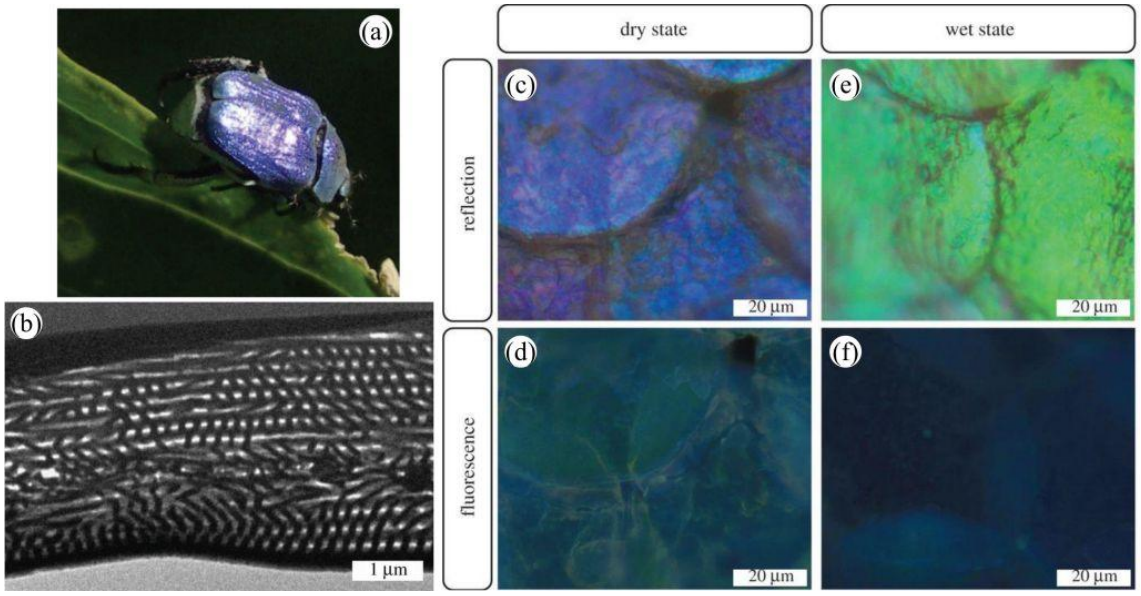

Figure 4: The blue-violet iridescent appearance of the male *H. coerulea* beetle (a) originates from a periodic photonic multilayer (b) located within the scales covering its body (c). Upon UV illumination, the fluorophores embedded in these scales exhibit a turquoise coloration (d). After immersion into water, the scales' color changes to green (e) when they are illuminated by visible white light and navy blue (f), under UV light. Reproduced from Mouchet, S.R., Lobet, M., Kolaric, B., Kaczmarek, A.M., Van Deun, R., Vukusic, P., Deparis, O., Van Hooijdonk, E., 2016. Controlled fluorescence in a beetle's photonic structure and its sensitivity to environmentally induced changes. Proc. R. Soc. B 283, 20162334.

electrical field ($\mathbf{E}(\omega)$), resulting in the following relation [57]:

$$\boldsymbol{\mu}(\omega) = \alpha(\omega)\mathbf{E}(\omega) \tag{1}$$

where $\alpha(\omega)$ represents the first-order polarizability, also called linear polarizability and ω is the frequency of the electromagnetic waves. Macroscopically, for the entire medium with a large number of molecules, all the induced dipole moments result in an induced polarization given $\mathbf{P}(\omega)$ by

$$\mathbf{P}(\omega) = \chi^{(1)}(\omega)\mathbf{E}(\omega) \tag{2}$$

with the first-order or linear susceptibility $\chi^{(1)}(\omega)$. However, when the light intensity is very high, this equation does not longer hold and the relation between the total polarization and the electric field is no longer linear. To account for this nonlinear correlation, the polarization is expanded in a Taylor series of the total applied electric field. This results in the equation:

$$\mathbf{P} = \mathbf{P}^{(1)} + \mathbf{P}^{(2)} + \mathbf{P}^{(3)} + ... = \chi^{(1)}\mathbf{E} + \chi^{(2)}\mathbf{EE} + \chi^{(3)}\mathbf{EEE} + ... \tag{3}$$

where $\mathbf{P}^{(1)}$, $\mathbf{P}^{(2)}$ and $\mathbf{P}^{(3)}$ are the linear, quadratic and cubic orders of electric field polarization, respectively. $\chi^{(2)}$ and $\chi^{(3)}$ represent respectively, the first- and the second-nonlinear susceptibilities, or the second- and third-order susceptibilities. These nonlinear susceptibilities are at the origin of nonlinear optical effects such as multiphoton excitation fluorescence and SHG [57].

A linear optical experiment example is the absorption of a photon with a specific wavelength and energy, resulting in the electronic and vibrational excitation of the material (Figure 5). After vibrational relaxation, the material gets back to a lower energy level while emitting a photon with a lower energy, such as in fluorescence emission, as exemplified in the previous section.

In the case of two-photon excitation fluorescence, which is a nonlinear effect, high intensity photons illuminate a sample. Because of the high intensity, two photons can simultaneously interact with the sample. Such an interaction is similar to one-photon fluorescence, however with different selection rules. Since two photons are absorbed initially and give rise to only one emitted photon, this resulting photon has a higher energy than each of the two absorbed photons.

In SHG, the investigated material also interacts with two photons. Unlike two-photon excitation fluorescence, a third photon will be instantaneously emitted. The two initially absorbed

This article is protected by copyright. All rights reserved.

Accepted Article

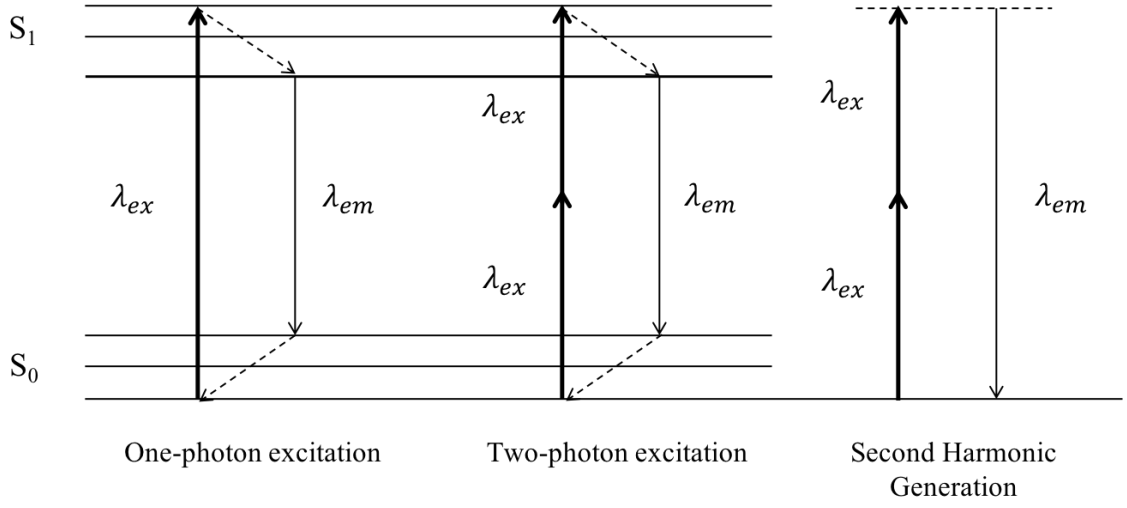

Figure 5: **Jablonski diagram of one- and two-photon excitation fluorescence, and Second Harmonic Generation (SHG)** Considering one-photon excitation fluorescence, one photon is absorbed which brings the molecule or the nanostructure from the ground state (S_0) to an excitated singlet state (S_1). Immediately (less than 10^{-12}s) internal conversion follows within the excited state, and the molecule falls back to the lowest vibrational state within S_1. A photon is emitted afterwards, leading the molecule back to its ground state S_0. Within S_0, the molecule is usually in an excited vibrational level. The molecule recovers its original energy state after another internal conversion. In the case of two-photon excitation fluorescence, two photons are absorbed simultaneously, after which internal relaxation follows. One single photon is emitted, with a higher energy than the two incident photons. In SHG, two photons interact simultaneously with the molecule or the nanostructure and excite it to a virtual state, via another virtual state. Immediately after the absorption (ca. 10^{-15}s), one photon, with the exact half wavelength (and thus the double energy) is emitted [58].

This article is protected by copyright. All rights reserved.

Accepted Article

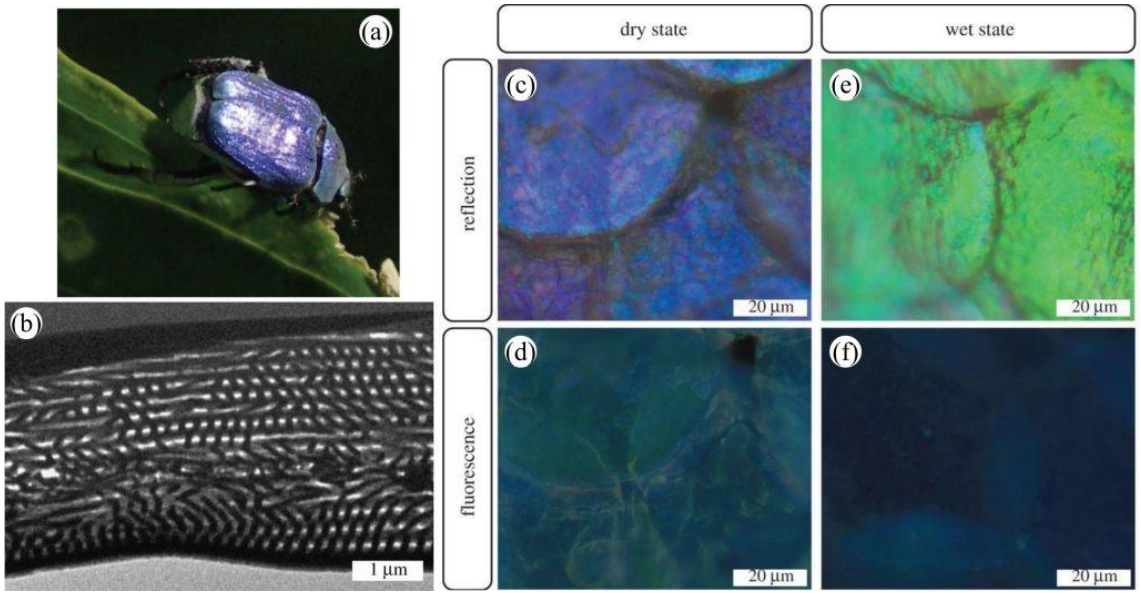

Figure 4: The blue-violet iridescent appearance of the male *H. coerulea* beetle (a) originates from a periodic photonic multilayer (b) located within the scales covering its body (c). Upon UV illumination, the fluorophores embedded in these scales exhibit a turquoise coloration (d). After immersion into water, the scales' color changes to green (e) when they are illuminated by visible white light and navy blue (f), under UV light. Reproduced from Mouchet, S.R., Lobet, M., Kolaric, B., Kaczmarek, A.M., Van Deun, R., Vukusic, P., Deparis, O., Van Hooijdonk, E., 2016. Controlled fluorescence in a beetle's photonic structure and its sensitivity to environmentally induced changes. Proc. R. Soc. B 283, 20162334.

electrical field ($\mathbf{E}(\omega)$), resulting in the following relation [57]:

$$\boldsymbol{\mu}(\omega) = \alpha(\omega)\mathbf{E}(\omega) \tag{1}$$

where $\alpha(\omega)$ represents the first-order polarizability, also called linear polarizability and ω is the frequency of the electromagnetic waves. Macroscopically, for the entire medium with a large number of molecules, all the induced dipole moments result in an induced polarization given $\mathbf{P}(\omega)$ by

$$\mathbf{P}(\omega) = \chi^{(1)}(\omega)\mathbf{E}(\omega) \tag{2}$$

with the first-order or linear susceptibility $\chi^{(1)}(\omega)$. However, when the light intensity is very high, this equation does not longer hold and the relation between the total polarization and the electric field is no longer linear. To account for this nonlinear correlation, the polarization is expanded in a Taylor series of the total applied electric field. This results in the equation:

$$\mathbf{P} = \mathbf{P}^{(1)} + \mathbf{P}^{(2)} + \mathbf{P}^{(3)} + ... = \chi^{(1)}\mathbf{E} + \chi^{(2)}\mathbf{EE} + \chi^{(3)}\mathbf{EEE} + ... \tag{3}$$

where $\mathbf{P}^{(1)}$, $\mathbf{P}^{(2)}$ and $\mathbf{P}^{(3)}$ are the linear, quadratic and cubic orders of electric field polarization, respectively. $\chi^{(2)}$ and $\chi^{(3)}$ represent respectively, the first- and the second-nonlinear susceptibilities, or the second- and third-order susceptibilities. These nonlinear susceptibilities are at the origin of nonlinear optical effects such as multiphoton excitation fluorescence and SHG [57].

A linear optical experiment example is the absorption of a photon with a specific wavelength and energy, resulting in the electronic and vibrational excitation of the material (Figure 5). After vibrational relaxation, the material gets back to a lower energy level while emitting a photon with a lower energy, such as in fluorescence emission, as exemplified in the previous section.

In the case of two-photon excitation fluorescence, which is a nonlinear effect, high intensity photons illuminate a sample. Because of the high intensity, two photons can simultaneously interact with the sample. Such an interaction is similar to one-photon fluorescence, however with different selection rules. Since two photons are absorbed initially and give rise to only one emitted photon, this resulting photon has a higher energy than each of the two absorbed photons.

In SHG, the investigated material also interacts with two photons. Unlike two-photon excitation fluorescence, a third photon will be instantaneously emitted. The two initially absorbed

This article is protected by copyright. All rights reserved.

Accepted Article

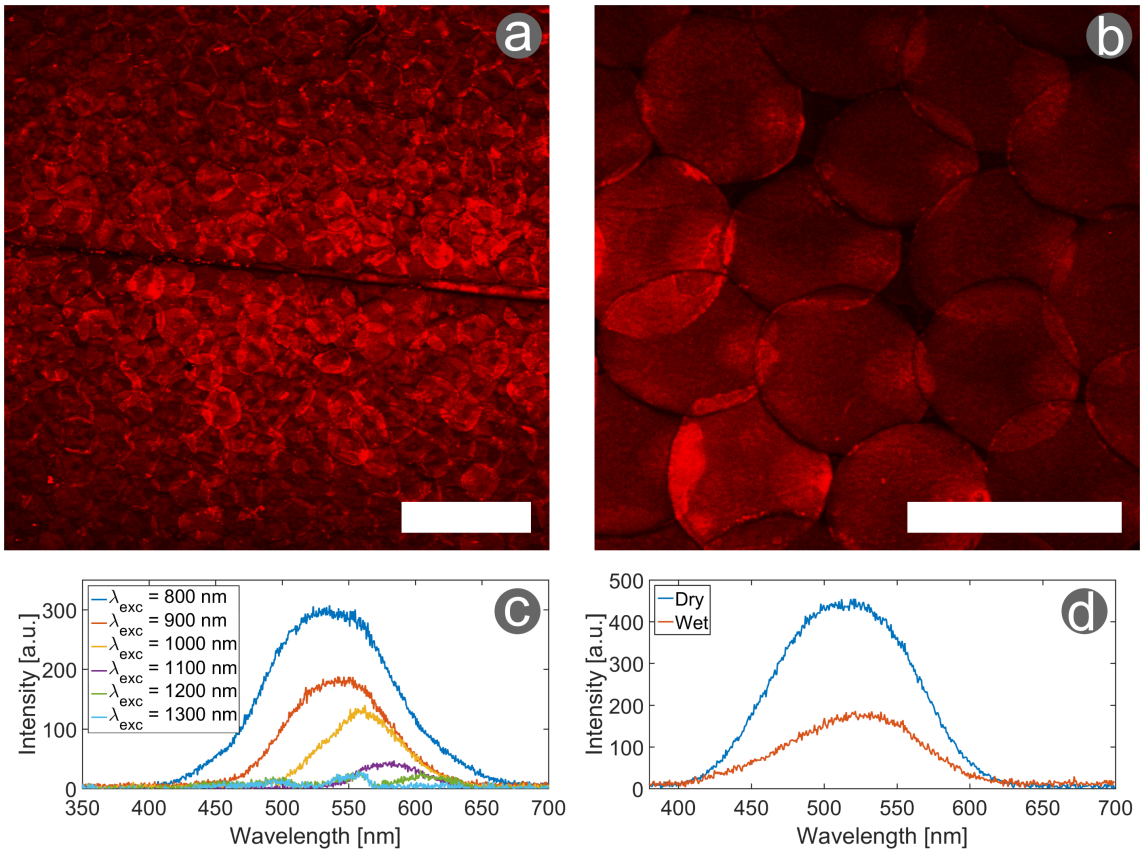

Figure 6: **Two-photon excitation fluorescence microscopy and spectroscopy of *H. coerulea*'s elytra.** The elytra of the male *H. coerulea* beetle show a strong TPEF response with excitation at (a) 900 nm and (b) 800 nm, resulting in clear image of the scales covering the beetle's elytra (with a 75 mW incident power). (c) At a low incident power (20 mW), The two-photon excitation fluorescence excitation spectra were measured with excitation wavelengths ranging between 800 and 1300 nm. (d) A small red-shift of the peak wavelength and a decrease in intensity is observed when the scale is put into contact with water. The excitation wavelength equals 800 nm, the incident power is 20 mW. Scale bars: (a) 200 μm and (b) 100 μm. Reproduced from [56].

This article is protected by copyright. All rights reserved.

Accepted Article

in the previous section [56]. It was further characterized with nonlinear optical methods. Due to the embedded fluorophores, two-photon excitation fluorescence was observed at a wide variety of wavelengths (Figure 6a-c). No SHG signal was measured, but it could be overshadowed by the strong two-photon excitation fluorescent signal. Additionally, the influence of water on the elytra was examined (Figure 6d). This resulted in a small red-shift and a strong decrease in signal intensity. This research thus provided a better insight in the photonic properties of *H. coerulea*'s elytra and its hygrochromic behavior (i.e., color change upon contact with water).

Although much useful information can be derived from these simple experiments, not many insect biological tissues have been characterized with multiphoton microscopy. Some other example are the two-pronged bristletails *Plusiocampa christiani* and *Pheggomisetes ninae* [84] as well as the the fire-chaser beetle *Melanophila acuminata* [85].

THG signal has been recently used in the investigation of fossilized teeth. The comparison between the dental anatomy of fossilized and currently living crocodilians provided with new insights in these species' evolution. The evolutionary signature of crocodilian teeth was found to be consistent over time [86].

4 Nonclassical Light for Super Resolution Quantum Imaging in Biological Systems

Besides the fact that at the most profound level, light is a purely quantum phenomenon, a majority of linear and nonlinear effects can be explained within the framework of classical physics [57].

Nonclassical light (quantum light) is the light which properties and interactions with matter can only be described using the formalism of quantum physics. The quantum light is used to beat the limitations of classical light regarding diffraction limit and signal-to-noise ratio which are essential requirements for biologically oriented research. The archetypes of nonclassical light are entangled and squeezed light [87, 88, 89, 90].

Quantum entanglement is a phenomenon in which a particle such as a photon exhibits a quantum state characterized e.g., by its energy or polarization, and cannot be described independently from the state of another particle even if these particles are separated by a significant distance. Measurements of physical properties such as position, momentum, spin, polarization and energy performed on entangled particles can be found to be correlated.

Entangled photons are generally generated by nonlinear processes such as Spontaneous Parametric Down-Conversion (SPDC) in which a beam of photons produced by a laser interacts with a nonlinear optical crystal or a nonlinear waveguide and spontaneously decays into pairs of correlated photons.

Since the first development of quantum physics, the entanglement is considered to be "the characteristic trait of quantum mechanics, the one that enforces its entire departure from classical lines of thought" [91][92]. This assessment was later confirmed by Bell's theorem [93] and the subsequent experiments, establishing that quantum entanglement gives rise to a certain kind of non-locality in nature.

The nonclassical nature of quantum entanglement has been employed in quantum technologies despite several fundamental difficulties: it is indeed very sensitive to decoherence, which generally accompanies interaction with the local environment. In addition, it is also limited by the so-called entanglement monogamy, which states that two particles in a maximally entangled state cannot be entangled with a third particle. As a consequence, it ultimately restricts the number of degrees of freedom involved in any related technique. However, one of the primary and most challenging goals [94, 92] of modern quantum research is to exploit quantum entanglement at ambient temperature and within the biological matter and to reveal links between classical and quantum dynamics in biologically consequential processes such as photosyntesis, signal recognition, navigation such as for migratory birds, etc. Since experiments of quantum light with biological matter are still at an infant stage, we present here some exciting examples which can be used to enhance quality of the image and signal-to-noise ratio using both entangled and squeezed quantum light.

Quantum imaging is indeed one of the most promising quantum applications in biologically oriented research. Improving optical imaging is essential since many natural photonic nanoarchitectures as described in section 2 as well as many subcellular structures are on length scales far below the diffraction limit of classical light [95]. Imaging such structures in situ and their inter-

This article is protected by copyright. All rights reserved.

Accepted Article

actions with different agents is the holy grail of modern biophysics and biophotonics. In the last ten years the possibility of manipulating single quantum states, in particular photons, has opened the possibility to develop technologies exploiting properties of quantum correlations for imaging purposes [87]. Here in this perspective articles the three most studied quantum imaging methods, namely Ghost Imaging (GI), Sub-Rayleigh Imaging (SRI) and squeezed light microscopy, will be briefly described.

4.1 Ghost Imaging

GI is the first so-called quantum imaging technique that attracted a huge interest of a broad scientific community. It exploits intensity correlation fluctuations for imaging an object. One spatially incoherent beam propagates through an object and is collected by a detector, called "bucket detector" that has no spatial resolution (Figure 7) [87][96]. The second correlated beam does not interact with the object and is collected by a spatially-resolved detector, made of an array of pixels. The image of the object is retrieved by measuring a correlation $S(x_j)$ coincidence between detectors (x_j being the position of the pixel j in the reference region). This result is significant since the image is reconstructed using the detected spatial information that did not actually interact with the object.

This article is protected by copyright. All rights reserved.

Accepted Article

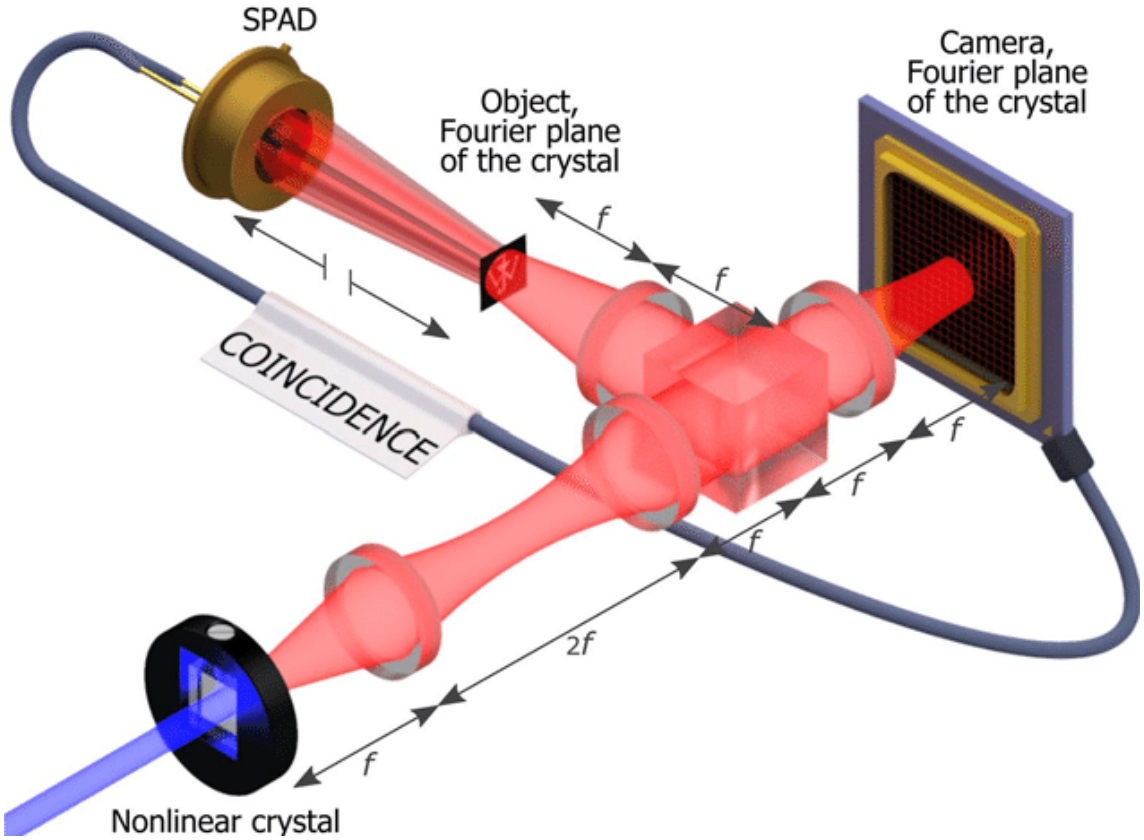

Figure 7: Schematic view of Quantum Ghost imaging setup, "Image plane" configuration. Correlated photons are generated in a nonlinear crystal pumped by an UV laser. The photons are separated by a beam splitter. The center of the crystal is imaged on both the object and the camera. In order to retrieve the ghost image, the coincidences between the single-photon avalanche diode (SPAD) and the camera are recorded. As indicated by the broken arrows the position of the SPAD relatively to the object is unimportant, the only requirement being that it collects the full light beam to act as a "bucket detector". Reproduced from [96] with permission of Wiley.

However, strictly speaking, GI does not represent a true quantum imaging protocol, since it can be performed without entangled light. Classical light GI has been widely employed in computational science to perform so-called computational ghost imaging recovery [97].

Besides the fact that GI does not require entangled light, it still presents an important advantage, offering significantly larger visibility in the presence of a diffusive medium, a condition important for recoding images in open air especially in the presence of fog (e.g., LIDAR application) or for imaging of biological samples where tissues represent the diffusive media [98] (Figure 8). It should be point out that in the Morris article [98], at the first time the imaging a real biophotonic structure, i.e., a wasp wing, using low numbers of entangled photons is fully described. Furthermore, Morris and coworkers showed that quantum GI techniques based on low photon number counting enable the successful reconstruction of images with less than one photon per pixel, which is an essential advantage for imaging biological processes in situ. In addition, using quantum light for GI significantly enhances the properties of various GI protocols [99, 100].

Furthermore, Zeilinger's group[100] exploits new entangled light protocols for optical imaging and clearly demonstrated the possibility to detect images at various wavelength ranges significantly improving signal-to-noise ratio with respect to classical imaging. The presented experiment is the archetype example in which quantum knowledge-information can be extracted from a system, even when photons are never detected. Zeilinger's protocol is the foundation for building a true quantum imaging system.

This article is protected by copyright. All rights reserved.

Accepted Article

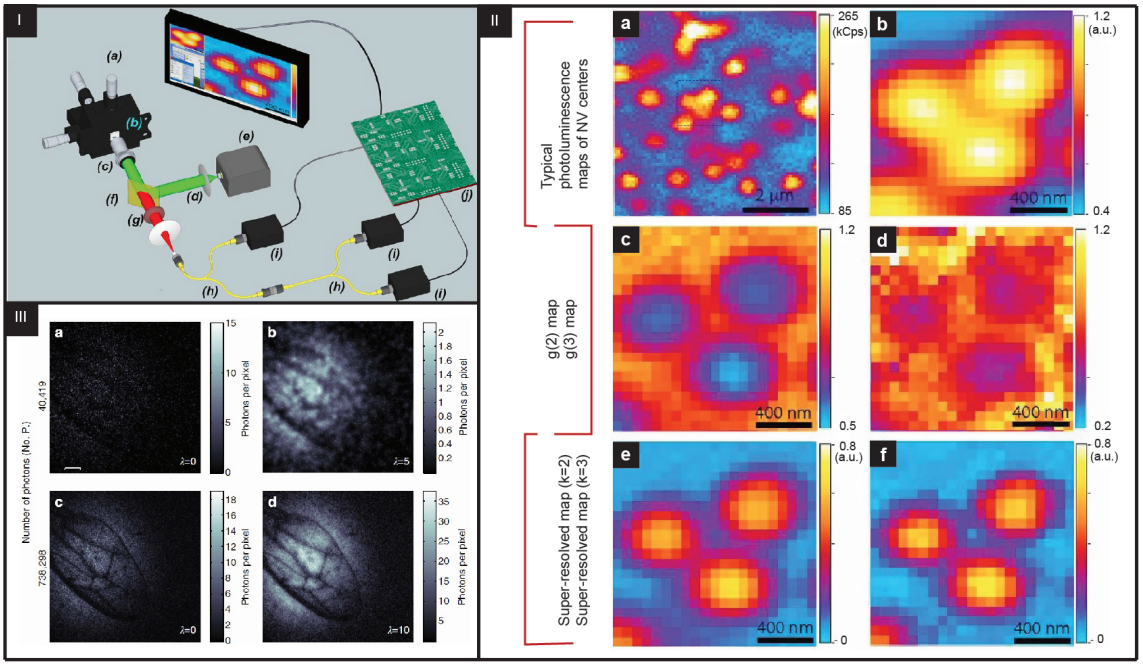

Figure 8: I) Schematic view of the experimental setup: (a) XYZ closed-loop piezoelectric stage, (b) sample, (c) 100×oil objective, (d) excitation light (532 nm), (e) laser source, (f) dichroic filter, (g) long-pass filters, (h) 50:50 fiber beam splitter, (i) single-photon detectors, and (j); II) Example of the super-resolution technique applied to a cluster of 3 NV centers. (a) Typical scan on a region of the sample obtained collecting the signals emitted by each center on a pixel-by-pixel basis via single-photon sensitive confocal microscope. (b) Magnification of the area of interest. (c) Map of $g(2)$ function. (d) Map of $g(3)$ function. (e) Super-resolved map for $k = 2$. (f) Super-resolved map for $k = 3$, III) Quantum image of a wasp wing at low photon number count. (a) Image of a wasp wing using 40,419 detected photons and (b) the corresponding reconstructed image. (c) An image of the same wasp wing with a greater number of photons and (d) its associated reconstructed image. Scale bar, 400 μm. Modified from [87, 101] and [98] with permission from APS Publishing and Springer Nature, respectively.

This article is protected by copyright. All rights reserved.

Accepted Article

4.2 Sub-Rayleigh Imaging

Recently, significant results in which the diffraction limit was beaten have been achieved exploiting emission properties of materials such as stimulated emission depletion (STED) and ground state depletion (GSD) [102]. These methods require very specific experimental conditions such as a dual laser excitation system, the presence of materials that allow luminescence quenching by stimulated emission and nontrivial shaping of the quenching beam. A possibility to overcome these limits is to use nonclassical correlations of quantum light, similar to GI. SRI can be viewed as the extension of the quantum ghost imaging technique that uses N quantum light sources with intensity measurements being replaced by N-fold coincidence detection strategies. By employing quantum light and coincidence measurements, the resolution is significantly enhanced [87].

A first step in SRI is to produce entangled photons by SPDC, to record the correlations between photons, like in the case of GI and to build an image based on these correlations. In the case when multi-entangled states are used with a higher number of entangled photons, the resolution is improved. However, due to the difficulties to produce multiphoton entanglement, a successful practical strategy relies on exploiting post-selection[1] to extract the "nonclassical component" from a classical state containing information about the object that is imaged. Several theoretical schemes have been proposed to achieve SRI [104].

Recently, super resolution was experimentally confirmed by illuminating an object with a laser and by post-selecting into arrays of single photon detectors. Note that pixels are generated only when photons are correlated, i.e., simultaneously detected. This example shows that with a unique and clever combination of nonclassical light and luminescent emission, it is possible to beat the diffraction limit to generate an image, only through correlations. This method reaches a sub-Rayleigh resolution improvement by a factor of $\ln \sqrt{(}N_{\max}/N)$.

[1]Post-selection is the selection of a subset of data, conditioned on the outcome of a certain measurement. For details, see reference [103].

This article is protected by copyright. All rights reserved.

Accepted Article

4.3 Squeezed Light

Recently, a different kind of nonclassical light, namely squeezed light, has been suggested in order to achieve improved resolution. The basic concept of squeezing emerges from the dynamics of a quantum harmonic oscillator [105, 106]. In most general descriptions, squeezed light can be defined as the light for which the noise of the electric field, i.e., the intensity fluctuations, and phases fall below the vacuum state.

The so-called squeezing factor R is related to the variances of the position and momentum, i.e., the intensity and the phase in the classical picture and determines the extent of the light squeezing. If $R > 1$, the position variance is below the vacuum state and the light intensity is squeezed (increased signal-to-noise ratio). In the case where $R < 1$, the squeezing of the phase is achieved. However, it is important to notice that in accordance with the uncertainty principle (i.e., both position and momentum not simultaneously observable) , the phase and intensity cannot be squeezed at the same time. That is illustrated in the next figure that shows the graphical representation of the squeezed light. Forty years ago, many studies related to squeezed light were published but without experimental realization of the squeezing. The first experimental signature of squeezed light was observed in a groundbreaking experiment of Slusher [107], using the process of four-wave-mixing in an atomic vapor of sodium atoms. Soon after the Slusher experiments, other approaches have been realized for generating squeezed light such as a fiber-based approach, exploiting the other nonlinear phenomena such as the third-order Kerr-type nonlinearity and second-order nonlinearity of a ferroelectric crystal. Recently, processes of PDC (parametric down conversion) and optical parametric oscillation (OPO) within a cavity are used to generate squeezed light. The first approaches to generate squeezed light are fully described elsewhere [107].

This article is protected by copyright. All rights reserved.

Accepted Article

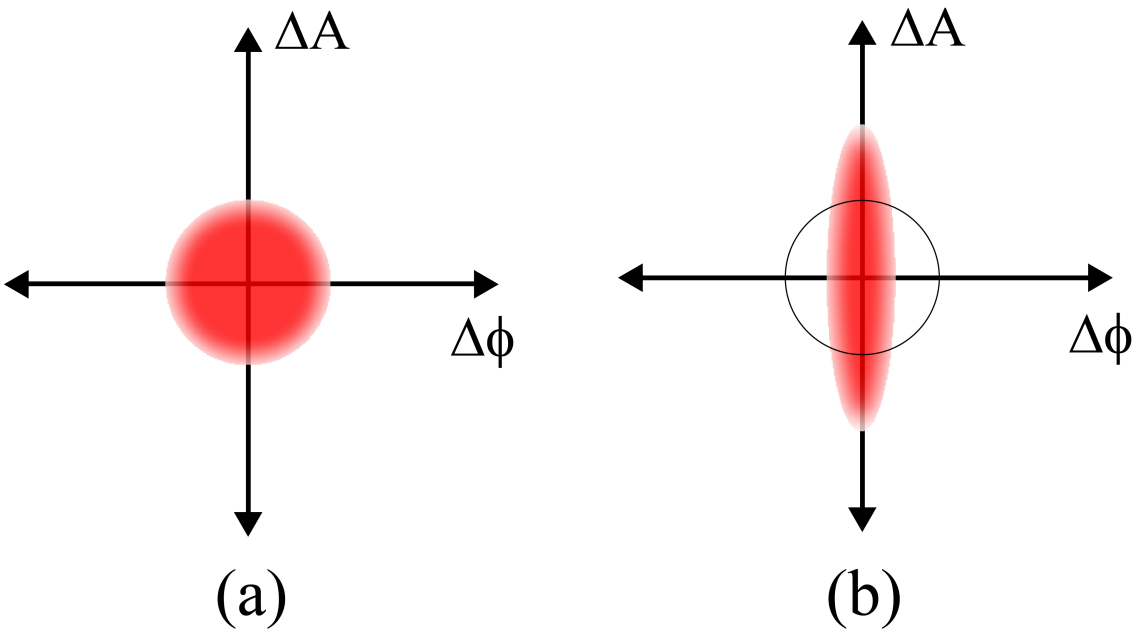

Figure 9: Schematic view of the quantum noise i.e., ball, showing the even distribution of uncertainty between the two quantities amplitude A and phase Φ (b) Squeezed noise, where the uncertainty in one quantity is less than quantum noise, while the other uncertainty is greater than quantum noise.

Significant advancements have been made from the initial 0.3 dB squeezing till today's near 15 dB squeezing. It is, however, interesting to point out that the experimental platforms to achieve squeezing, i.e.,nonlinear crystals, fibers and atomic ensembles used in the late eighties are almost the same as those used today for generating highly efficient squeezing [108],[105, 106] Beyond the physical significance .of generating and characterizing squeezed light, squeezed light microscopy, also called photonic force microscopy (PFM), has recently been developed by Taylor *et al.* [90] for fast and accurate sub-shot noise measurements, i.e., tracking of (polymers and bipolymers) particles (Figure 10).

This article is protected by copyright. All rights reserved.

Accepted Article

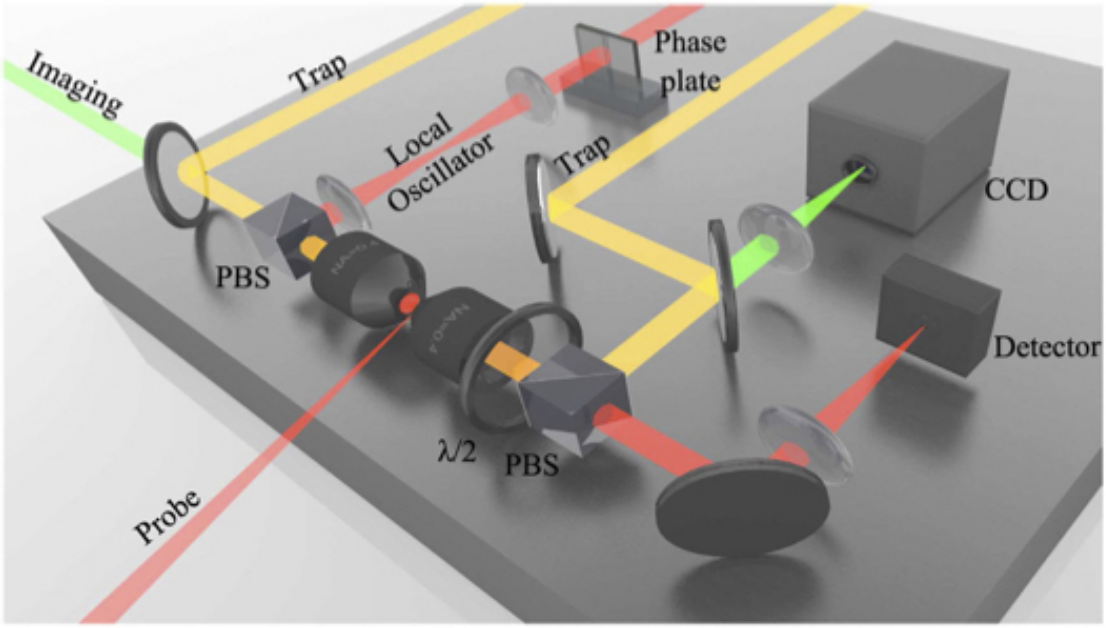

Figure 10: Squeezed light microscopy. Motion of a particle near the focus is tracked with an amplitude-squeezed local oscillator and an amplitude-modulated probe (red). The probe provides dark-field illumination, with the particle tracking signal arising from interference between scattered light from the probe and the local oscillator. Particles are also manipulated with trapping fields (yellow), and visualized on a CCD camera using an imaging field (green). Reproduced from [90] with permission of SAPS.

The experiments performed by Taylor's group showed that subcellular structures as small as 10 nm can be observed by its local influence on the thermal motion of nanoparticles. This is striking since up to now the same resolution can only be achieved by a state-of-the-art atomic force microscopy. It should be pointed out that optical quantum enhanced particle tracking using squeezed light holds increasing relevance, with a wide range of potential applications in biology, from microrheology improving sensitivity of the viscoelastic response of the medium, to revealing the properties of the cytoplasm and biological processes at higher frequency [90]. More generally, the use of nonclassical squeezed light could enhance significantly a wide range of biological measurements techniques, such as two-photon microscopy, super-resolution and absorption imaging. Furthermore, the combination of a squeezed light source with different optical resonator geometries allows not only sub-noise tracking of particles but also possibilities to determine the shape and structure of the tracked particles.

5 Conclusions

In this perspective article, we present the state of the art of linear and nonlinear optical studies of various biophotonic and biological structures using classical light. The importance of biophotonic studies for the biomedical community is especially emphasized in this article. We also present a short overview of quantum light and its potential (and most profound) applications in current biology-oriented research. Although quantum light has a large advantage over classical light, due to breaking the diffraction limit, real quantum experiments in bio-optics are still far away from realization and real-life applications. One of the reasons for that is the lack of synergy between physicists and biologists. The primary aim of this article is to attract the interest of the broad biological community for the biophotonics and experiments with quantum light, which could be used to open new horizons in biologically oriented research. The synergy and cooperations between physicists, biologists and physicians could open the door for new groundbreaking applications of quantum techniques in biology and medicine. This progress article is one of the first small steps

This article is protected by copyright. All rights reserved.

Accepted Article

in that direction.

Acknowledgements S.R.M. was supported by the Belgian National Fund for Scientific Research (FRS-FNRS) as a Postdoctotal Researcher (91400/1.B.309.18F). T.V. acknowledges financial support from the Hercules Foundation. B.K. acknowledges financial support from the "Action de Recherche Concertée" (BIOSTRUCT project, No.10/15-033) of UNamur, from Nanoscale Quantum Optics COST-MP1403 action and from FRS-FNRS; Interuniversity Attraction Pole: Photonics@be (P7-35, Belgian Science Policy Office). The authors warmly acknowledge Mrs. Bojana Bokic, Institute of Physics, the University of Belgrade for the assistance in editing some images for publication.

References

[1] Shuichi Kinoshita. *Structural Colors in the Realm of Nature*. World Scientific Publishing Co, Singapore, 2008.

[2] Ainsley E Seago, Parrish Brady, Jean-Pol Vigneron, and Tom D Schultz. Gold bugs and beyond: a review of iridescence and structural colour mechanisms in beetles (coleoptera). *Journal of The Royal Society Interface*, 6(Suppl 2):S165–S184, 2009.

[3] Sébastien R Mouchet and Pete Vukusic. Structural colours in lepidopteran scales. *Advances in Insect Physiology*, 54:1–53, 2018.

[4] Craig I Peter and Steven D Johnson. Mimics and magnets: the importance of color and ecological facilitation in floral deception. *Ecology*, 89(6):1583–1595, 2008.

[5] B. R. Wooten and G. A. Geri. Psychophysical determination of intraocular light scatter as a function of wavelength. *Vision Research*, 27(8):1291–1298, 1987.

[6] Richard O. Prum and Rodolfo H. Torres. Structural colouration of mammalian skin: convergent evolution of coherently scattering dermal collagen arrays. *Journal of Experimental Biology*, 207(12):2157–2172, 2004.

[7] Crawford H. Greenewalt, Werner Brandt, and Daniel D. Friel. Iridescent colors of hummingbird feathers. *J. Opt. Soc. Am.*, 50(10):1005–1013, Oct 1960.

[8] Haiwei Yin, Lei Shi, Jing Sha, Yizhou Li, Youhua Qin, Biqin Dong, Serge Meyer, Xiaohan Liu, Li Zhao, and Jian Zi. Iridescence in the neck feathers of domestic pigeons. *Phys. Rev. E*, 74:051916, Nov 2006.

[9] Shinya Yoshioka, Eri Nakamura, and Shuichi Kinoshita. Origin of two-color iridescence in rock dove's feather. *Journal of the Physical Society of Japan*, 76(1):013801, 2007.

[10] L.P. Biró and J.P. Vigneron. Photonic nanoarchitectures in butterflies and beetles: valuable sources for bioinspiration. *Laser & Photonics Reviews*, 5(1):27–51, 2011.

[11] Andrew Zangwill. *Modern Electrodynamics*. Cambridge University Press, 2013.

[12] P R Stoddart, P J Cadusch, T M Boyce, R M Erasmus, and J D Comins. Optical properties of chitin: surface-enhanced raman scattering substrates based on antireflection structures on cicada wings. *Nanotechnology*, 17(3):680, 2006.

[13] Mingxia Sun, Aiping Liang, Yongmei Zheng, Gregory S Watson, and Jolanta A Watson. A study of the anti-reflection efficiency of natural nano-arrays of varying sizes. *Bioinsp. Biomim.*, 6(2):026003, 2011.

[14] Louis Dellieu, Michaël Sarrazin, Priscilla Simonis, Olivier Deparis, and Jean-Pol Vigneron. A two-in-one superhydrophobic and anti-reflective nanodevice in the grey cicada *Cicada orni* (hemiptera). *Journal of Applied Physics*, 116(2):024701, 2014.

[15] Olivier Deparis, Sébastien R. Mouchet, Louis Dellieu, Jean-François Colomer, and Michaël Sarrazin. Nanostructured surfaces: Bioinspiration for transparency, coloration and wettability. *Materials Today: Proceedings*, 1S:122–129, 2014.

This article is protected by copyright. All rights reserved.

Accepted Article

[16] C. G. Bernhard, W. H. Miller, and A. R. Møller. The insect corneal nipple array. *Acta Physiol. Scand.*, 63 (Suppl. 243):1–25, 1965.

[17] D.G Stavenga, S Foletti, G Palasantzas, and K Arikawa. Light on the moth-eye corneal nipple array of butterflies. *Proceedings of the Royal Society of London B: Biological Sciences*, 273(1587):661–667, 2006.

[18] Olivier Deparis, Nadia Khuzayim, Andrew Parker, and Jean-Pol Vigneron. Assessment of the antireflection property of moth wings by three-dimensional transfer-matrix optical simulations. *Phys. Rev. E*, 79:041910, Apr 2009.

[19] R.H. Siddique, G. Gomard, and H. Hölscher. The role of random nanostructures for the omnidirectional anti-reflection properties of the glasswing butterfly. *Nat. Commun.*, 6:6909, 2015.

[20] D.G. Stavenga. Thin film and multilayer optics cause structural colors of many insects and birds. *Mater. Today Proc.*, 1S:109–121, 2014.

[21] Akihiro Yoshida, Mayumi Motoyama, Akinori Kosaku, and Kiyoshi Miyamoto. Nanoprotuberance array in the transparent wing of a hawkmoth, *Cephonodes hylas. Zoological science*, 13(4):525–526, 1996.

[22] Akihiro Yoshida, Mayumi Motoyama, Akinori Kosaku, and Kiyoshi Miyamoto. Antireflective nanoprotuberance array in the transparent wing of a hawkmoth, *Cephonodes hylas. Zoological science*, 14(5):737–741, 1997.

[23] Akihiro Yoshida. Antireflection of the butterfly and moth wings through microstructure. *Forma*, 17(2):75–89, sep 2002.

[24] Guoyong Xie, Guoming Zhang, Feng Lin, Jin Zhang, Zhongfan Liu, and Shichen Mu. The fabrication of subwavelength anti-reflective nanostructures using a bio-template. *Nanotechnology*, 19(9):095605, 2008.

[25] Z.W. Han, Z. Wang, X.M. Feng, B. Li, Z.Z. Mu, J.Q. Zhang, S.C. Niun, and L.Q. Ren. Antireflective surface inspired from biology: A review. *Biosurface and Biotribology*, 2:137–150, 2016.

[26] Mingxia Sun, Gregory S. Watson, Yongmei Zheng, Jolanta A. Watson, and Aiping Liang. Wetting properties on nanostructured surfaces of cicada wings. *Journal of Experimental Biology*, 212(19):3148–3155, 2009.

[27] Katrina M. Wisdom, Jolanta A. Watson, Xiaopeng Qu, Fangjie Liu, Gregory S. Watson, and Chuan-Hua Chen. Self-cleaning of superhydrophobic surfaces by self-propelled jumping condensate. *Proceedings of the National Academy of Sciences*, 110(20):7992–7997, 2013.

[28] Elena P. Ivanova, Jafar Hasan, Hayden K. Webb, Vi Khanh Truong, Gregory S. Watson, Jolanta A. Watson, Vladimir A. Baulin, Sergey Pogodin, James Y. Wang, Mark J. Tobin, Christian Löbbe, and Russell J. Crawford. Natural bactericidal surfaces: Mechanical rupture of *Pseudomonas aeruginosa* cells by cicada wings. *Small*, 8(16):2489–2494, 2012.

[29] Elena P. Ivanova, Jafar Hasan, Hayden K. Webb, Gediminas Gervinskas, Saulius Juodkazis, Vi Khanh Truong, Alex H.F. Wu, Robert N. Lamb, Vladimir A. Baulin, Gregory S. Watson, Jolanta A. Watson, David E. Mainwaring, and Russell J. Crawford. Bactericidal activity of black silicon. *Nature Communications*, 4:2838, nov 2013.

[30] S. M. Kelleher, O. Habimana, J. Lawler, B. O'Reilly, S. Daniels, E. Casey, and A. Cowley. Cicada wing surface topography: An investigation into the bactericidal properties of nanostructural features. *ACS Applied Materials & Interfaces*, 8(24):14966–14974, 2016. PMID: 26551558.

[31] Felix Vüllers, Guillaume Gomard, Jan B. Preinfalk, Efthymios Klampaftis, Matthias Worgull, Bryce Richards, Hendrik Hölscher, and Maryna N. Kavalenka. Bioinspired superhydrophobic highly transmissive films for optical applications. *Small*, 12(44):6144–6152, 2016.

This article is protected by copyright. All rights reserved.

Accepted Article

[32] Mathias Kolle, Alfred Lethbridge, Moritz Kreysing, Jeremy J. Baumberg, Joanna Aizenberg, and Peter Vukusic. Bio-inspired band-gap tunable elastic optical multilayer fibers. *Advanced Materials*, 25(15):2239–2245, 2013.

[33] Silvia Vignolini, Thomas Gregory, Mathias Kolle, Alfie Lethbridge, Edwige Moyroud, Ullrich Steiner, Beverley J. Glover, Peter Vukusic, and Paula J. Rudall. Structural colour from helicoidal cell-wall architecture in fruits of *Margaritaria nobilis*. *Journal of The Royal Society Interface*, 13(124), 2016.

[34] Joanna Aizenberg, Mathias Kolle, Peter Vukusic, and Robert D. Howe. Band-gap tunable elastic optical multilayer fibers, December 17 2015. US 2015/0362669 A1.

[35] Matthew Jacobs, Martin Lopez-Garcia, O.-Phart Phrathep, Tracy Lawson, Ruth Oulton, and Heather M. Whitney. Photonic multilayer structure of *Begonia* chloroplasts enhances photosynthetic efficiency. *Nature Plants*, 2:16162, 2016.

[36] H. L. Gorton and T. C. Vogelmann. Effects of epidermal cell shape and pigmentation on optical properties of antirrhinum petals at visible and ultraviolet wavelengths. *Plant Physiology*, 112(3):879–888, 1996.

[37] Dimitrios Gkikas, Apostolos Argiropoulos, and Sophia Rhizopoulou. Epidermal focusing of light and modelling of reflectance infloral-petals with conically shaped epidermal cells. *Flora*, 2212:38–45, 2015.

[38] Ruben Hünig, Adrian Mertens, Moritz Stephan, Alexander Schulz, Benjamin Richter, Michael Hetterich, Michael Powalla, Uli Lemmer, Alexander Colsmann, and Guillaume Gomard. Flower power: Exploiting plants' epidermal structures for enhanced light harvesting in thin-film solar cells. *Advanced Optical Materials*, 4(10):1487–1493, 2016.

[39] Raphael Schmager, Benjamin Fritz, Ruben Hünig, Kaining Ding, Uli Lemmer, Bryce S. Richards, Guillaume Gomard, and Ulrich W. Paetzold. Texture of the *Viola* flower for light harvesting in photovoltaics. *ACS Photonics*, 4(11):2687–2692, 2017.

[40] C. Neinhuis and W. Barthlott. Characterization and distribution of water-repellent, self-cleaning plant surfaces. *Annals of Botany*, 79(6):667–677, 1997.

[41] W. Barthlott and C. Neinhuis. Purity of the sacred lotus, or escape from contamination in biological surfaces. *Planta*, 202(1):1–8, Apr 1997.

[42] Victoria L. Welch, Eloise Van Hooijdonk, Nurit Intrater, and Jean-Pol Vigneron. Fluorescence in insects. *Proc.SPIE*, 8480:8480 – 8480 – 15, 2012.

[43] M. Gabriela Lagorio, Gabriela. B. Cordon, and Analia Iriel. Reviewing the relevance of fluorescence in biological systems. *Photochem. Photobiol. Sci.*, 14:1538–1559, 2015.

[44] Justin Marshall and Sonke Johnsen. Fluorescence as a means of colour signal enhancement. *Philosophical Transactions of the Royal Society of London B: Biological Sciences*, 372(1724), 2017.

[45] E. M. Purcell. Spontaneous emission probabilities at radio frequencies. *Phys. Rev.*, 69:681, 1946.

[46] E. Yablonovitch. Inhibited spontaneous emission in solid-state physics and electronics. *Physical Review Letters*, 58:2059–2062, 1987.

[47] Jean-Pol Vigneron, Jean-François Colomer, Nathalie Vigneron, and Virginie Lousse. Natural layer-by-layer photonic structure in the squamae of *Hoplia coerulea* (coleoptera). *Phys. Rev. E*, 72:061904, Dec 2005.

[48] S.R. Mouchet, M. Lobet, B. Kolaric, A.M. Kaczmarek, R. Van Deun, P. Vukusic, O. Deparis, and E. Van Hooijdonk. Photonic scales of *Hoplia coerulea* beetle: any colour you like. *Mater. Today Proc.*, 4:4979–4986, 2017.

This article is protected by copyright. All rights reserved.

Accepted Article

[49] Eloise Van Hooijdonk, Serge Berthier, and Jean-Pol Vigneron. Bio-inspired approach of the fluorescence emission properties in the scarabaeid beetle *Hoplia coerulea* (coleoptera): Modeling by transfer-matrix optical simulations. *Journal of Applied Physics*, 112(11):114702, 2012.

[50] Sébastien R. Mouchet, Michaël Lobet, Branko Kolaric, Anna M. Kaczmarek, Rik Van Deun, Peter Vukusic, Olivier Deparis, and Eloise Van Hooijdonk. Controlled fluorescence in a beetle's photonic structure and its sensitivity to environmentally induced changes. *Proceedings of the Royal Society of London B: Biological Sciences*, 283(1845), 2016.

[51] Marie Rassart, Priscilla Simonis, Annick Bay, Olivier Deparis, and Jean-Pol Vigneron. Scale coloration change following water absorption in the beetle hoplia coerulea (coleoptera). *Phys. Rev. E*, 80:031910, Sep 2009.

[52] Sébastien R. Mouchet, Bao-Lian Su, Tijani Tabarrant, Stéphane Lucas, and Olivier Deparis. *Hoplia coerulea*, a porous natural photonic structure as template of optical vapour sensor. *Proceedings of SPIE*, 9127(91270U), 2014.

[53] Sébastien R. Mouchet, Tijani Tabarrant, Stéphane Lucas, Bao-Lian Su, Pete Vukusic, and Olivier Deparis. Vapor sensing with a natural photonic cell. *Opt. Express*, 24(11):12267–12280, May 2016.

[54] S.R. Mouchet, E. Van Hooijdonk, V.L. Welch, P. Louette, J.-F. Colomer, B.-L. Su, and O. Deparis. Liquid-induced colour change in a beetle: the concept of a photonic cell. *Sci. Rep.*, 6:19322, 2016.

[55] S.R. Mouchet, E. Van Hooijdonk, V.L. Welch, P. Louette, T. Tabarrant, P. Vukusic, S. Lucas, J.-F. Colomer, B.-L. Su, and O. Deparis. Assessment of environmental spectral ellipsometry for characterising fluid-induced colour changes in natural photonic structures. *Mater. Today Proc.*, 4:4987–4997, 2017.

[56] Sébastien R Mouchet, Charlotte Verstraete, Dimitrije Mara, Stijn Van Cleuvenbergen, Ewan D Finlayson, Rik Van Deun, Olivier Deparis, Thierry Verbiest, Bjorn Maes, Pete Vukusic, and Branko Kolaric. Non-linear optical spectroscopy and two-photon excited fluorescence spectroscopy reveal the excited states of fluorophores embedded in beetle's elytra. *arXiv preprint arXiv:1801.07639*, 2018.

[57] Thierry Verbiest, Koen Clays, and Vincent Rodriguez. *Second-order nonlinear optical characterization techniques: an introduction*. CRC press, 2009.

[58] Joseph Lakowizc. *Principles of Fluorescence Spectroscopy, 3rd Edition*. Kluwer Academic, 2006.

[59] Winfried Denk, James H Strickler, and Watt W Webb. Two-photon laser scanning fluorescence microscopy. *Science*, 248(4951):73–76, 1990.

[60] Jörg Bewersdorf, Rainer Pick, and Stefan W Hell. Multifocal multiphoton microscopy. *Optics letters*, 23(9):655–657, 1998.

[61] Warren R Zipfel, Rebecca M Williams, and Watt W Webb. Nonlinear magic: multiphoton microscopy in the biosciences. *Nature biotechnology*, 21(11):1369, 2003.

[62] Guy Cox and Colin JR Sheppard. Practical limits of resolution in confocal and non-linear microscopy. *Microscopy research and technique*, 63(1):18–22, 2004.

[63] Andrew M Smith, Michael C Mancini, and Shuming Nie. Bioimaging: second window for in vivo imaging. *Nature nanotechnology*, 4(11):710, 2009.

[64] Peter Friedl, Katarina Wolf, Gregory Harms, and Ulrich H. Andrian. Biological second and third harmonic generation microscopy. *Current Protocols in Cell Biology*, 34(1):4.15.1–4.15.21, 2007.

[65] Ryan S. Ries, Hyeon Choi, Rikard Blunck, Francisco Bezanilla, and James R. Heath. Black lipid membranes: visualizing the structure, dynamics, and substrate dependence of membranes. *The Journal of Physical Chemistry B*, 108(41):16040–16049, 2004.

This article is protected by copyright. All rights reserved.

Accepted Article

[66] Trang T. Nguyen and John C. Conboy. High-throughput screening of drug–lipid membrane interactions via counter-propagating second harmonic generation imaging. *Analytical Chemistry*, 83(15):5979–5988, 2011. PMID: 21696170.

[67] Patrick Theer, Winfried Denk, Mordechai Sheves, Aaron Lewis, and Peter B. Detwiler. Second-harmonic generation imaging of membrane potential with retinal analogues. *Biophysical Journal*, 100(1):232–242, 2011.

[68] Jasper Akerboom, Nicole Carreras Calderón, Lin Tian, Sebastian Wabnig, Matthias Prigge, Johan Tolö, Andrew Gordus, Michael Orger, Kristen Severi, John Macklin, Ronak Patel, Stefan Pulver, Trevor Wardill, Elisabeth Fischer, Christina Schüler, Tsai-Wen Chen, Karen Sarkisyan, Jonathan Marvin, Cornelia Bargmann, Douglas Kim, Sebastian Kügler, Leon Lagnado, Peter Hegemann, Alexander Gottschalk, Eric Schreiter, and Loren Looger. Genetically encoded calcium indicators for multi-color neural activity imaging and combination with optogenetics. *Frontiers in Molecular Neuroscience*, 6:2, 2013.

[69] Donald J. Brown, Naoyuki Morishige, Aneesh Neekhra, Don S. Minckler, and James V. Jester. Application of second harmonic imaging microscopy to assess structural changes in optic nerve head structure ex vivo. *Journal of Biomedical Optics*, 12:12 – 12 – 5, 2007.

[70] Xiyi Chen, Oleg Nadiarynkh, Sergey Plotnikov, and Paul J Campagnola. Second harmonic generation microscopy for quantitative analysis of collagen fibrillar structure. *Nature protocols*, 7(4):654, 2012.

[71] Gloria A Di Lullo, Shawn M Sweeney, Jarmo Körkkö, Leena Ala-Kokko, and James D San Antonio. Mapping the ligand-binding sites and disease-associated mutations on the most abundant protein in the human, type i collagen. *Journal of Biological Chemistry*, 277(6):4223–4231, 2002.

[72] David JS Hulmes. Building collagen molecules, fibrils, and suprafibrillar structures. *Journal of structural biology*, 137(1-2):2–10, 2002.

[73] Yao Liu, Xiaoqin Zhu, Zufang Huang, Jianyong Cai, Rong Chen, Shuyuan Xiong, Guannan Chen, and Haishan Zeng. Texture analysis of collagen second-harmonic generation images based on local difference local binary pattern and wavelets differentiates human skin abnormal scars from normal scars. *Journal of biomedical optics*, 20(1):016021, 2015.

[74] Kirby R Campbell and Paul J Campagnola. Assessing local stromal alterations in human ovarian cancer subtypes via second harmonic generation microscopy and analysis. *Journal of biomedical optics*, 22(11):116008, 2017.

[75] Matthew W Conklin, Jens C Eickhoff, Kristin M Riching, Carolyn A Pehlke, Kevin W Eliceiri, Paolo P Provenzano, Andreas Friedl, and Patricia J Keely. Aligned collagen is a prognostic signature for survival in human breast carcinoma. *The American journal of pathology*, 178(3):1221–1232, 2011.

[76] Nathaniel D Kirkpatrick, Molly A Brewer, and Urs Utzinger. Endogenous optical biomarkers of ovarian cancer evaluated with multiphoton microscopy. *Cancer Epidemiology and Prevention Biomarkers*, 16(10):2048–2057, 2007.

[77] LH Li, WZ Jiang, DY Kang, X Liu, HS Li, GX Guan, SM Zhuo, ZF Chen, and JX Chen. Second-harmonic imaging microscopy for identifying colorectal intraepithelial neoplasia. *Journal of microscopy*, 2018.

[78] Carrie K Hui Mingalone, Zhiyi Liu, Judith M Hollander, Kirsten D Garvey, Averi L Gibson, Rose E Banks, Ming Zhang, Timothy E McAlindon, Heber C Nielsen, and Irene *et al.* Georgakoudi. Bioluminescence and second harmonic generation imaging reveal dynamic changes in the inflammatory and collagen landscape in early osteoarthritis. *Laboratory Investigation*, page 1, 2018.

[79] Suman Ranjit, Evgenia Dobrinskikh, John Montford, Alexander Dvornikov, Allison Lehman, David J Orlicky, Raphael Nemenoff, Enrico Gratton, Moshe Levi, and Seth Furgeson. Label-free fluorescence lifetime and second harmonic generation imaging microscopy improves quantification of experimental renal fibrosis. *Kidney international*, 90(5):1123–1128, 2016.

This article is protected by copyright. All rights reserved.

Accepted Article

[80] Gaël Latour, Laurianne Robinet, Alexandre Dazzi, François Portier, Ariane Deniset-Besseau, and Marie-Claire Schanne-Klein. Correlative nonlinear optical microscopy and infrared nanoscopy reveals collagen degradation in altered parchments. *Scientific Reports*, 6:26344, 2016.

[81] Meng Han, Günter Giese, and Josef F. Bille. Second harmonic generation imaging of collagen fibrils in cornea and sclera. *Opt. Express*, 13(15):5791–5797, Jul 2005.

[82] Paul J Campagnola, Andrew C Millard, Mark Terasaki, Pamela E Hoppe, Christian J Malone, and William A Mohler. Three-dimensional high-resolution second-harmonic generation imaging of endogenous structural proteins in biological tissues. *Biophysical journal*, 82(1):493–508, 2002.

[83] Kirby Campbell, Rajeev Chaudhary, Julia Handel, Manish Patankar, and Paul J Campagnola. Shg polarization resolved analysis of ovarian cancer. In *Novel Techniques in Microscopy*, pages NW3C–3. Optical Society of America, 2017.

[84] Mihailo D Rabasović, Dejan V Pantelić, Branislav M Jelenković, Srećko B Ćurčić, Maja S Rabasović, Maja D Vrbica, Vladimir M Lazović, Božidar PM Ćurčić, and Aleksandar J Krmpot. Nonlinear microscopy of chitin and chitinous structures: a case study of two cave-dwelling insects. *Journal of Biomedical Optics*, 20(1):016010, 2015.

[85] Meir Israelowitz, Syed HW Rizvi, and Herbert P von Schroeder. Fluorescence of the "fire-chaser" beetle *Melanophila acuminata*. *Journal of luminescence*, 126(1):149–154, 2007.

[86] Yu-Cheng Chen, Szu-Yu Lee, Yana Wu, Kirstin Brink, Dar-Bin Shieh, Timothy D Huang, Robert R Reisz, and Chi-Kuang Sun. Third-harmonic generation microscopy reveals dental anatomy in ancient fossils. *Optics letters*, 40(7):1354–1357, 2015.

[87] Marco Genovese. Real applications of quantum imaging. *J. Opt.*, 18(073002):10, 2016.

[88] Manuel Unternährer, Bänz Bessire, Leonardo Gasparini, Matteo Perenzoni, and André Stefanov. Super-resolution quantum imaging at the heisenberg limit. *CLEO: QELS Fundamental Science*, 2018.

[89] Laurent Olislager, Wakana Kubo, Takuo Tanaka, Simona Ungureanu, Renaud A. L. Vallée, Branko Kolaric, Philippe Emplit, and Serge Massar. Propagation and survival of frequency-bin entangled photons in metallic nanostructures. *Nanophotonics*, 4:324–331, 2015.

[90] Michael A. Taylor, Jiri Janousek, Vincent Daria, Joachim Knittel, Boris Hage, Hans-A. Bachor, and Warwick P. Bowen. Subdiffraction-limited quantum imaging within a living cell. *Phys.Rev.X*, 4:011017, 2014.

[91] Erwin Schrödinger. *Science and the human temperament*. Allen & Unwin, 1935.

[92] Branko Kolaric, Bjorn Maes, Koen Clays, Thomas Durt, and Yves Caudano. Strong light-matter coupling as a new tool for molecular and material engineering: Quantum approach. *Advanced Quantum technologies, doi.org/10.1002/qute.201800001*, 2018.

[93] Tristan Kraft, Christina Ritz, Nicolas Brunner, Marcus Huber, and Otfried Gühne. Characterizing genuine multilevel entanglement. *Physical Review Letters*, 120:0605020, 2009.

[94] Thomas Juffmann Thomas Arndt and Vlatko Vedral. Quantum physics meets biology. *HFSP journal*, 3:386–400, 2009.

[95] Olaf Karthaus. *Biomimetics in Photonics*. CRC press, 2013.

[96] Paul-Antoine Moreau, Ermes Toninelli, Thomas Gregory, and Miles J. Padgett. Ghost imaging using optical correlations. *Laser Photonics Rev. 2017*, 12:1700143, 2017.

[97] J. Shapiro. Computational ghost imaging. *Phys. Rev. A*, 78, 2008.

[98] Peter A. Morris, Reuben S. Aspden, Jessica E.C. Bell, Robert W. Boyd, and Miles J. Padgett. Imaging with a small number of photons. *Nature Communications*, 6, 2015.

This article is protected by copyright. All rights reserved.

Accepted Article

[99] Qiang Wang *et al.* Super-resolving quantum lidar: entangled coherent-state sources with binary-outcome photon counting measurement suffice to beat the shot-noise limit. *Optical Express*, 24(5):5045, 2016.

[100] Gabriela B. Lemos, Victoria Borish, Garrett D. Cole, Sven Ramelow, Radek Lapkiewicz, and Anton Zeilinger. Quantum imaging with undetected photons. *Nature Photonics*, 512, 2014.

[101] D. Gatto Monticone et al. Beating the abbe diffraction limit in confocal microscopy via nonclassical photon statistic. *Phys.Rev.Lett*, 113, 2014.

[102] Sunae So *et al.* Overcoming diffraction limit: From microscopy to nanoscopy. *Journal of Applied Spectroscopy Reviews*, 53, 2018.

[103] Mirko Cormann, Mathilde Remy, Branko Kolaric, and Yves Caudano. Revealing geometric phases in modular and weak values with a quantum eraser. *Physical Review A*, 93, 2016.

[104] Lorenzo Maccone Vittorio Giovannetti, Seth Lloyd. Advances in quantum metrology. *Nature Photonics*, 5:222–229, 2011.

[105] A. I Lvovsky. Squeezed light. *Arxiv,/arxiv.org/abs/1401.4118*, 2016.

[106] Ulrik L Andersen et al. 30 years of squeezed light generation. *Phys. Scr*, 2016.

[107] SR. E. Slusher, L. W. Hollberg, B. Yurke, J. C. Mertz, and J. F. Valley. Observation of squeezed states generated by four-wave mixing in an optical cavity. *Physical review Letters*, 56, 1986.

[108] Karsten Danzmann Roman Schnabel Henning Vahlbruch, Moritz Mehmet. Detection of 15 db squeezed states of light and their application for the absolute calibration of photoelectric quantum efficiency. *Phys. Rev. Lett.*, 117(110801), 2016.

This article is protected by copyright. All rights reserved.